Comparative measurement of the breakup length of liquid jets in airblast atomisers using optical connectivity, electrical connectivity and shadowgraphy

Georgios Charalampous[1*], Constantinos Hadjiyiannis[1], Yannis Hardalupas[1]

[1] Department of Mechanical Engineering, Imperial College London, London, SW7 2AZ, UK

[*]Corresponding author: georgios.charalampous@imperial.ac.uk, Tel: +44(0)20 7594 5788

Abstract

A comparative examination of the optical connectivity, electrical connectivity and shadowgraphy techniques for the measurement of the break-up length of atomising liquid jets from a co-axial airblast atomiser is presented. The atomiser was operated over air-to-liquid Momentum Ratios between 27 and 335 and Momentum Flux Ratios between 0.67 and 8.27. Shadowgraphy records instantaneous images of the shadow of the atomising liquid jet when it is back-illuminated by a light source. The electrical connectivity uses the continuity of an electrically conducting atomising liquid jet to measure the potential during the presence of an electrical connection between the spray nozzle and a probe further downstream. The optical connectivity visualises the atomising liquid jet, doped with a fluorescing dye, as it is illuminated from within the nozzle using a laser beam. Comparison of the measured breakup lengths with time resolved shadowgraphy, optical connectivity and electrical connectivity, following the proposed novel processing of the time-dependent potential, showed that the mean values are all within ±15% of each other. The advantages and limitations of each technique are discussed.

Keywords

Liquid atomisation
Optical Connectivity
Electrical Connectivity
Shadowgraphy
Liquid Breakup length

1. Introduction

The atomisation of liquid jets by injection in a gaseous environment is a process, which is utilised in many practical applications, such as automotive and aviation engines, agricultural sprays, dust control, firefighting and nuclear reactor core cooling. The atomisation process is complex and several parameters, such as the physical properties and the flow characteristics of both the injected liquid and of the surrounding air and the geometry of the atomiser, contribute to the formation of the final spray. However, the importance of all the influencing parameters is not known. Yet, there is high demand for precise control of the spray characteristics. For example, the injected liquid fuel in a burner must atomise quickly near the nozzle to form small droplets, which disperse well into the surrounding air, so that they evaporate quickly and mix with the air to improve fuel consumption and reduce combustion emissions. A lubricating liquid jet on the other hand needs to maintain coherence for some distance beyond the nozzle, so that the lubricant is delivered to the precise location it is required in order to reduce its consumption and avoid contamination of surrounding areas.

The control of the spray characteristics requires a deeper understanding of the atomisation process, which is broken down in smaller sub-processes that can be independently examined and understood. The most fundamental description of the atomisation process follows a two stage approach, namely the primary and the secondary atomisation [1, 2]. Primary atomisation begins immediately at the nozzle exit, where destabilising forces operate on the gas-liquid interface to break up the continuous liquid stream into discrete liquid fragments. The liquid jet usually maintains continuity for several liquid jet diameters downstream of the nozzle exit. After the continuity of the liquid jet is interrupted, secondary atomisation takes place, which involves further breakup of the liquid fragments into progressively smaller sizes until stable droplets are obtained. This complex process involves many spatial and temporal scales. One of the key spatial scales is the length of the continuous liquid jet past the nozzle exit, which is known as the “breakup length”. The breakup length is critical because it defines the spatial extent of the primary atomisation region. The measurement of the breakup length is therefore crucial in spray studies, because it is essential for the physics of atomisation and the performance of atomisers [3-6] and for the evaluation of computational models for atomisation [7].

A number of techniques have been developed for the measurement of the break-up length. The most prominent is photography. It is the most widely used method [6, 8-11], because it is straightforward to apply, it places only moderate demands on equipment and the photographic images provide detailed information of the continuous liquid geometry. In this method, the atomising liquid jet is imaged directly by a camera. An intense and fast light source is required to illuminate the liquid jet, so that the exposure time is short compared to the time scales of atomisation in order for the jet image to remain sharp. The liquid jet may be illuminated from different directions, but usually back illumination is preferred (Shadowgraphy). In this way, the shadow of the jet is recorded against a bright background,

delivering high contrast images where the liquid jet contour is well defined. The shadowgraphy technique is extensively presented in [12] where a theoretical analysis on the formation of the shadow of the visualised object is provided and the capabilities of shadowgraphic visualisation are highlighted. Shadowgraphy facilitates the visualisation of the whole liquid jet from which many morphological characteristics can be extracted, including the breakup length. While this method is easy to implement and gives good results under certain flow conditions, it has the disadvantage that, when atomisation becomes intense and the density of droplets around the liquid jet increases, the optical access to the liquid jet core is reduced. In this case, there is poor jet visualisation and, therefore, ambiguity in the estimate of the break-up length and other liquid jet characteristics.

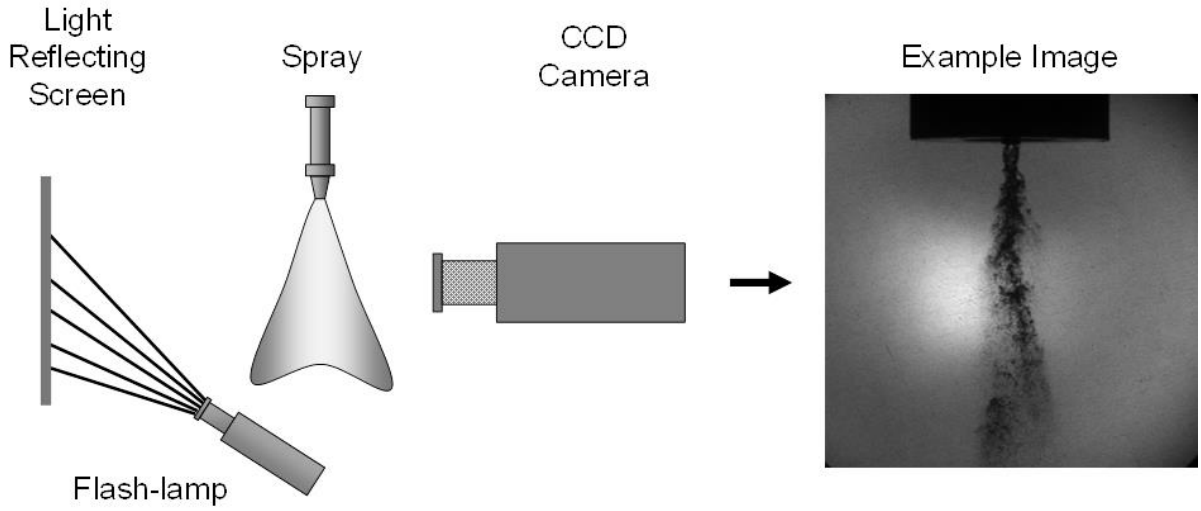

Fig 1. Principle of photographic spray imaging using shadowgraphy

A different approach for the measurement of the breakup length is the electrical connectivity technique, which does not rely on the visualisation of the continuous liquid jet and, therefore, does not share the same difficulties. This technique is based on the conduction of electricity along the length of the continuous liquid jet downstream of the nozzle. A potential is applied between the spray nozzle and a probe downstream. If there is continuity of the liquid phase between the nozzle and the probe, a closed electrical circuit will ensue. The probe can be moved across different positions to determine the continuity of the liquid jet as a function of the downstream distance. If the measured potential between the nozzle and the probe is low, then there is electrical connectivity between the two, indicating continuity of the liquid jet core. Discontinuity of the liquid jet can be inferred when the measured potential between the nozzle and the probe is high. The theoretical basis of the electrical connectivity method was developed in the seminal work of Hiroyasu et al [13]. A theoretical analysis of the expected measured potential between the needle probe and the nozzle was performed by Chehroudi et al [14] and Yule and Salters [15]. These

authors consider the continuous liquid jet as a resistor. Therefore, the jet resistance increases with the jet length and decreases with the jet cross sectional area and consequently the measured potential across the nozzle and the probe. Various morphologies of the continuous liquid jet core were examined from which its resistance is estimated. However, no consensus exists on the expected output signal behaviour among authors, since different assumptions were made on the shape of the jet. Additionally, there are differences in the implementation of the technique between different researchers. Hiroyasu et al. studied the breakup length of a high-speed liquid jet by measuring an electrical resistance between the nozzle and a fine wire screen detector located in a spray jet [13]. Chehroudi et al. tried to determine the shape and length of the intact liquid core by applying a voltage between the nozzle unit and fine needles, rods and screens [14]. Their results indicate that electrical current can be transmitted, not only by continuous liquid cores, but, also, by atomised unconnected liquid fragments, which would represent a serious limitation for the technique. Yule and Salters investigated the breakup zone of a transient diesel spray as a function of time and position employing a wire probe [15]. For this reason a visual inspection of the process is necessary in order to assess how the measured potential should be interpreted.

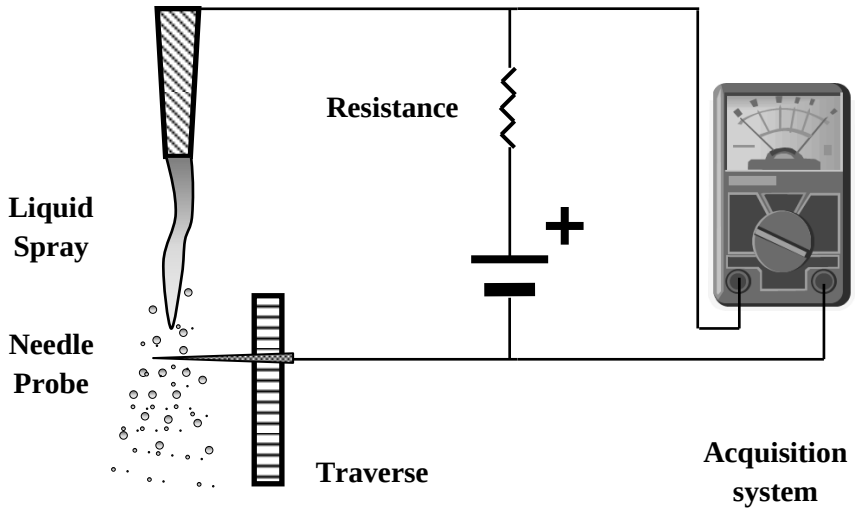

Fig 2. Principle of the electrical connectivity technique

A novel technique for the measurement of the break-up length was recently proposed by Charalampous et al [16, 17], which is based on the optical connectivity of a continuous liquid jet and aims at addressing some of the shortcomings of shadowgraphy and electrical connectivity. In this approach, the liquid jet is illuminated from within the nozzle by a laser beam. The beam propagates along the liquid jet by reflecting at the gas-liquid interface. Due to the higher index of refraction of the liquid jet to that of the surrounding gas, when the incident angle of the laser beam rays on the gas-liquid interface, defined from the normal to the interface, is greater than the angle for total internal reflection (about 48° for water), the laser beam is reflected completely back into the liquid stream and

propagates downstream for a long distance, in the same way that light propagates along optical fibers. This phenomenon was demonstrated as early as the 19th century [18, 19]. The addition of a fluorescent dye, such as Rhodamine WT [20] in the liquid jet, causes some of the intensity of the laser beam to be absorbed and re-emitted at a longer wavelength as fluorescence. This causes the volume of the continuous jet to become luminous, which allows the evaluation of the break-up length. Beyond the point of liquid discontinuity, the laser beam is diffused and its intensity is significantly reduced. A schematic of the process is shown in Fig 3. An extension of the theoretical principle is related to the propagation of the laser beam within a continuous liquid jet and the subsequent fluorescent emission from the continuous liquid jet. This has been performed numerically for ideal jet geometries [21]. It is found that in straight jets, such as those observed in coaxial airblast atomisers considered here, the laser beam can propagate sufficiently to illuminate liquid jets over 10 liquid nozzle diameters. This numerical investigation was expanded for instantaneous liquid jet geometries derived from Large Eddy Simulations of liquid jets in an air coflow [22], which were close to observed jet geometries under intense atomisation regime (We=1040 and MR=336). It was found that the laser beam can illuminate the full length of the liquid jet with some fluorescent intensity decrease close to the tip, where the jets become narrower. This technique offers the unique advantage that the continuous liquid jet is visualised without significant interference from the surrounding droplets and, therefore, does not suffer from the same issues as shadowgraphy. As such, the breakup length can be resolved in cases where atomisation is intense and shadowgraphy fails. These are the cases of significant interest as in most practical applications intense atomisation for the generation of fine droplets is required. There is a limitation of the jet length that can be visualised using optical connectivity, as light intensity losses by refraction occur at the jet interface. Nevertheless, this issue is mitigated by the fact that optical connectivity is useful for cases where atomisation is intense. In such cases, the continuous liquid jet length is short and the visualisation of the full jet length with optical connectivity is successful.

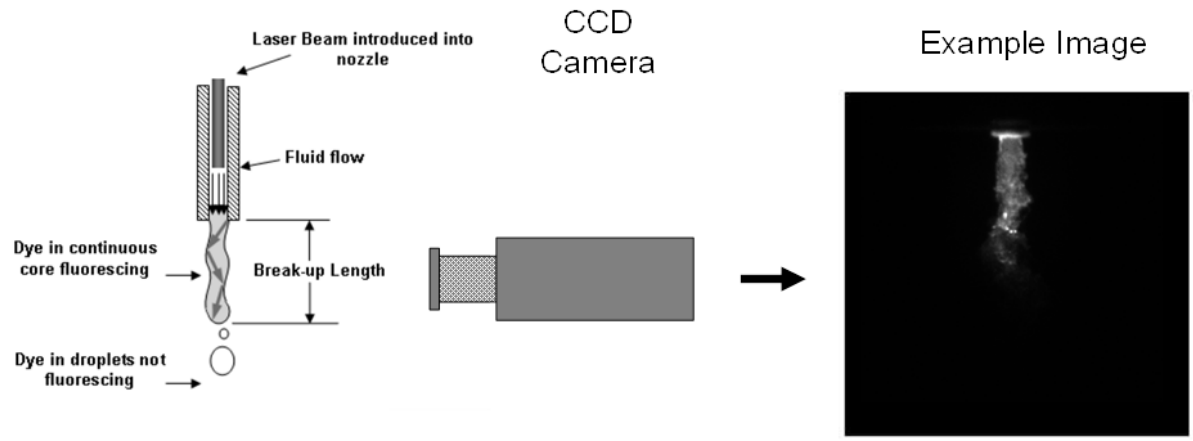

Fig 3. Principle of the optical connectivity technique

Other techniques exist for the measurement of the breakup length, such as X-ray absorption [23-25] and ballistic imaging [26-29]. While these techniques are powerful, they require advanced optical instrumentation, which is not commonly available in an engineering laboratory. Additionally, complicated experimental arrangements make these techniques unavailable to most researchers at present, while additional evaluation of their measurement accuracy is required. It is the purpose of this paper to provide a comparison between the measurement of the breakup length of a liquid jet by shadowgraphic imaging, electrical connectivity and optical connectivity, which can be implemented in most research laboratories. Different processing methods of measured data using the electrical connectivity technique are evaluated and the best approach is proposed.

The remaining of the paper is structured in the following sections. In the next section, the details of the experimental configuration of the tested co-axial airblast atomiser are presented along with the description of the implementation of each of the three considered techniques. The evaluation of data processing approaches of the electrical connectivity signals and the description of the results and their interpretation follows in Section 3. Section 4 presents a discussion of the results where the merits and weaknesses of each of the tested techniques are exposed. The paper ends with a summary of the conclusions.

2. Experimental set-up

The investigation was conducted on the liquid jet injected by the air-blast atomiser of Fig 4. The internal and external diameters of the liquid nozzle were D_L=2.3mm and 2.95mm respectively and the internal diameter of the gas nozzle was D_G=14.95mm. The length of the liquid nozzle was over $20D_L$ which ensures that the mean velocity profile of the liquid jet is sufficiently developed, while the gas nozzle had a contraction with an area ratio of about 30. The two working fluids were water and air. The atomiser was set up vertically and exhausted downwards in order to avoid complexities due to gravitational effects that would cause the liquid jet to deflect from a straight path. The flow rate of the water and the air was controlled by and measured using rotameters. The resolution of the water rotameter was 0.1 l/min while the resolution of the air rotameter was 50 l/min. Corrections were applied to the measured air flow rate to account for compressibility effects due to the increased pressure of the air supply. All measurements were obtained at room temperature and pressure.

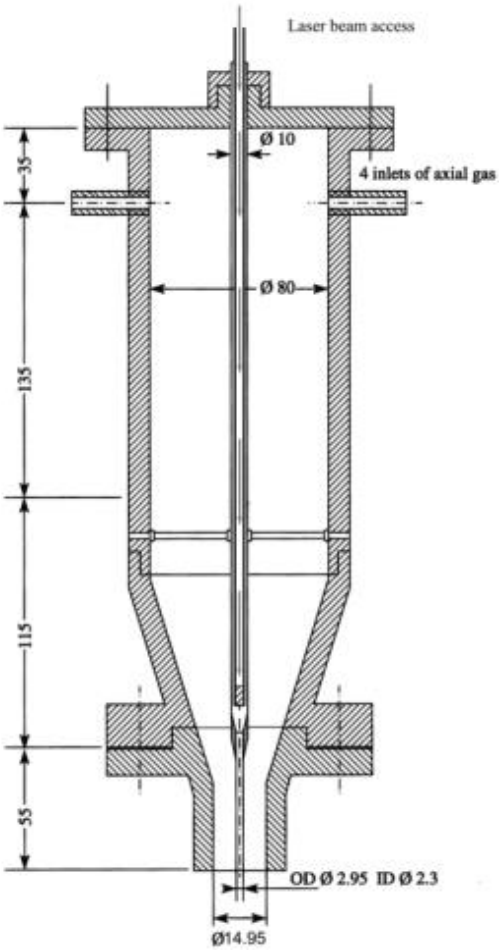

Fig 4. Geometry of coaxial air-blast atomiser

The shadowgraphic imaging measurements were performed with a 10-bit Photron Fastcam-APX RS high speed CMOS camera. The camera was fitted with a 105mm lens and the imaged region was resolved within approximately 30μm per pixel, resulting to a spatial resolution of about 75px over the

diameter of the liquid jet at the nozzle exit. Therefore, the liquid jet breakup length can be resolved in increments smaller than 5% of D_L. The camera frame acquisition rate was set to 20000 frames/s for all flow conditions. This frequency is greater than the breakup frequency of the liquid jet core for all tested flow conditions. As such, temporally resolved image sequences were recorded for each flow condition. The purpose of acquiring temporally resolved image sequences was to examine the possibility of improving the accuracy of the determination of the location of the liquid break-up in cases where the full length of the atomising jet is not clearly visible. This corresponds to flow conditions for which the products of atomisation obstruct the direct optical access to the liquid jet. If the liquid jet images are uncorrelated, the ambiguity can not be overcome. However, the breaking point of the liquid jet could be traced upstream from a temporal sequence of correlated images. The source of illumination was a 100W lamp that was placed behind the liquid jet, so that the shadow of the liquid jet was imaged in the forward scattering direction.

The measurements with the electrical connectivity technique were performed with a stainless needle probe with 1.1mm diameter, which crossed the axis of the atomiser. The probe was sufficiently robust to withstand the impact of the liquid without deflection as verified by shadowgraphy. The needle probe was supported on a robust beam to minimise vibrations. The distance between the needle probe and the nozzle was adjusted by a vertical traverse in steps of 1mm from the nozzle exit. This is sufficient to resolve the breakup length in increments of up to 40% of D_L. The spatial resolution of the electrical connectivity was not as fine as that of shadowgraphy. The current setup was appropriate to deliver spatial resolution of the breakup length measurements better than half the liquid jet diameter, which is more than adequate for the purposes of this investigation and a good compromise between spatial resolution and measurement time. An electrical circuit was designed (Fig 2) to measure the electrical potential between the nozzle and the probe. A constant voltage of 10V from a stabilised battery supply was applied between the liquid nozzle of the atomiser and the probe. The 10V electrical potential was selected because it offers a natural scale to compare the measurements and, as shown previously, the results of the technique do not depend on the applied electrical potential in the range between 6V and 60V [15]. The positive pole of the power supply was connected to the needle probe in series with a 1 MΩ resistance to regulate the current in the circuit. The negative pole of the power supply was wired straight to the nozzle of the atomiser. A low potential between the nozzle and the probe indicates good electrical connectivity and, therefore, continuity of the liquid jet. Conversely, a high potential between the two indicates poor electrical connectivity and, therefore, marginal continuity or complete discontinuity of the liquid jet. An analogue oscilloscope was used to monitor the potential between the nozzle and the probe, while acquisition of the potential was performed by a 12-bit analogue to digital converter (National Instruments PCI-6023E) capable of sampling at 200kHz. However, the sampling rate of the electrical connectivity was set at 20kHz, so that the electrical

connectivity measurements could be synchronised to the camera of the high speed shadowgraphic measurements for simultaneous measurements.

The measurements of the breakup length with the optical connectivity technique were reported elsewhere [16]. However, they are used here for comparison purposes. The details of the technique have been described elsewhere, however, we provide here a brief summary of the implementation of the technique. A stainless steel light guiding tube with a quartz window was inserted into the tube that delivers the liquid jet to the nozzle. The beam from a Nd:YAG laser, operating at 532nm, was steered into the light guiding tube by a system of mirrors and lenses, so that it entered in a direction parallel to the tube axis to minimise reflections on the internal surfaces of the tube. The laser beam exited just before the contraction of the liquid jet nozzle (see Fig 4), in a direction parallel to the nozzle axis, so that it follows the liquid stream. The atomising liquid was doped with Rhodamine WT dye, which is excited by laser light at 532nm and fluoresces strongly with a peak at 587nm. As a consequence, the liquid jet became luminous along the length of propagation of the beam. An Andor Classic iCCD camera was used to record images of the fluorescent liquid jet. A long pass optical filter that absorbs the laser wavelength at 532nm and transmits the longer wavelengths of the fluorescent light was placed in front of the camera lens to suppress scattered light. The optical connectivity measurements were not temporally resolved.

Simultaneous measurements of electrical connectivity and high speed shadowgraphic imaging were obtained for conditions with liquid jet area-averaged velocity of U_L=2.0m/s and annular flow area-averaged air velocities of U_G=47m/s, 71m/s, 95m/s, 119m/s, 142m/s and 166m/s. For the optical connectivity technique, the same liquid jet of U_L=2.0m/s was examined under U_G=47m/s, 71m/s, 119m/s and 166m/s. The operating conditions of the atomiser are considered in terms of the Reynolds number, Re, the Weber number, We, the momentum ratio, MR, and the momentum flux ratio, which are defined as:

$$\mathrm{Re} = \frac{\rho_L U_L D_L}{\mu} \tag{1}$$

$$We = \frac{\rho_G \left(U_L - U_G\right)^2 D_L}{\sigma} \tag{2}$$

$$MR = \frac{\rho_G}{\rho_L} \cdot \frac{U_G^2}{U_L^2} \cdot \frac{\left(D_G^2 - D_L^2\right)}{D_L^2} \tag{3}$$

$$MFR = \frac{\rho_G}{\rho_L} \cdot \frac{U_G^2}{U_L^2} \tag{3}$$

where ρ_L is the liquid density, ρ_G is the gas density, D_L is the internal diameter of the liquid nozzle, D_G is the internal diameter of the gas nozzle exit, U_L is the area-averaged velocity of the liquid at the nozzle exit, U_G is the area-average velocity of the annular gas flow at the nozzle exit, μ is the liquid dynamic viscosity and σ is the surface tension of the liquid. It should be noted that since the dimensions of the nozzle have not been changed here, the effects of MR and MFR cannot be distinguished. However, there are cases where the momentum flux may not suffice to describe the flow. If the continuous liquid jet extends beyond the potential core of the annular gas jet, the final stages of breakup occur under a decreased gas velocity. This has been pointed out by Engelbert et al [9] and, more recently, by [30]. In such cases, the diameter of the gas nozzle will have an effect on the resulting sprays, as confirmed by Matas and Cartellier [9]. For completeness, we have presented both the MR and MFR values.

The resulting liquid Reynolds number was 5442, while the Weber number ranged between 80 and 1041, the momentum flow ratio was between 27 and 335 and the momentum flux ratios between 0.67 and 8.27. For this range of flow conditions the breakup frequency of the liquid core of this atomiser is below 2000KHz [9] which is ten times lower than the sampling rate used in the present investigation and the sampling rate used for the high speed measurements is more than adequate to temporally resolve the breakup of the liquid jet. A summary of the tested conditions is presented in Table 1.

Table 1. Considered flow conditions of the co-axial airblast atomiser

U_L (m/s)	U_G (m/s)	Re	We	MR	MFR
2.0	47	5442	80	27	0.67
2.0	71	5442	185	61	1.52
2.0	95	5442	334	109	2.70
2.0	119	5442	526	171	4.22
2.0	142	5442	762	246	6.07
2.0	166	5442	1041	335	8.27

3. Evaluation of Data Processing approaches and Results

The results from each of the considered techniques are presented in this section. The methodology for the evaluation of the breakup length for the shadowgraphic imaging measurements and the electrical connectivity is also presented here. The methodology for the optical connectivity has been presented at a previous publication [16].

3.1. Shadowgraphic imaging

Example images from each of the flow conditions considered here are shown in Fig 5. Atomisation can be observed to progress from a destabilisation regime of the main jet at low MR to the stripping of droplets from the jet surface at high MR. It is possible to evaluate many aspects of the morphology of the liquid jet, such as the waves on the surface of the jet, the shape of the detached liquid, the flapping of the liquid jet and the breakup length.

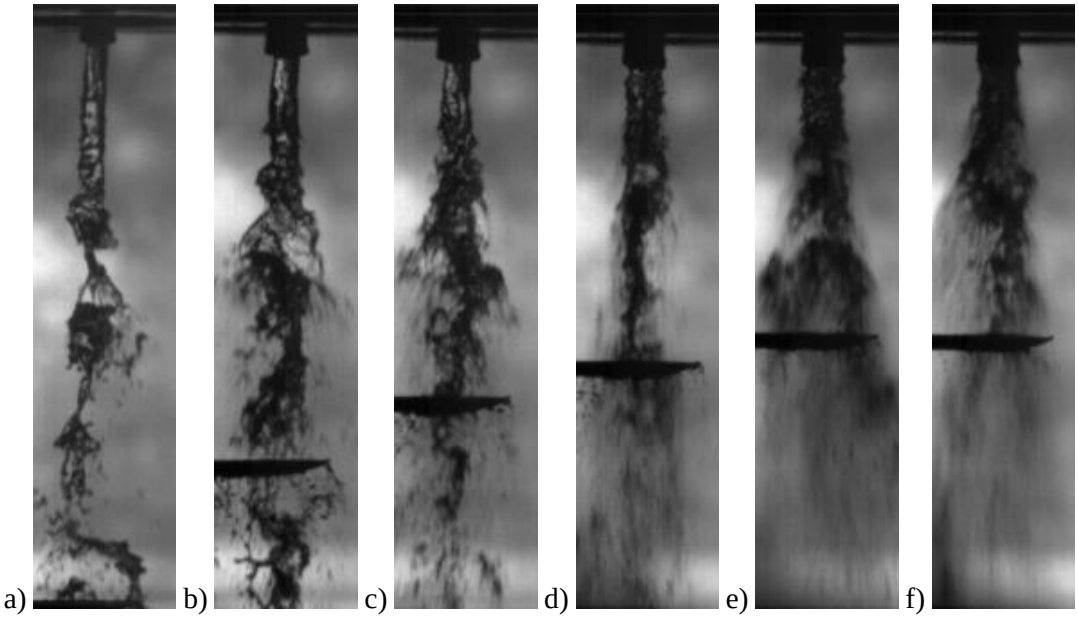

Fig 5. Examples of the shadowgraphic jet morphology for all the considered flow conditions. a) MR=27, b) MR=61, c) MR=109, d) MR=171, e) MR=246 and f) MR=335. The horizontal dark line is the electrical connectivity probe.

The evaluation of the breakup point from shadowgraphic images is a matter of interpretation. This is because it is not always possible to identify clearly the location of the breaking point. One issue is the presence of ligaments and lamella that can connect detached masses of liquid with the main liquid jet that is injected from the nozzle. This can be observed in all cases in Fig 5. For example in Fig 5a, the liquid jet breaks up in a succession of liquid fragments. While the continuity of the liquid jet is interrupted at about the middle of the image, there is a fine webbing of liquid ligaments that connect the main jet with the liquid fragment directly downstream. The same is true for the case of the most intense atomisation of Fig 5f, where, at the location of the breakup point half way between the nozzle

exit and the needle probe, fine ligaments connect the main jet with the detached segment downstream. This fine interconnection between successive liquid masses not only causes problems in the interpretation of the breakup length, but also makes the automated treatment of the liquid jet images unreliable, since thresholding of the image intensity will not correctly identify the main jet and lead to longer measured breakup lengths.

Another difficulty with shadowgraphy is that the detached liquid droplets and ligaments can obscure the observation of the breakup point. This type of ambiguity is demonstrated in Fig 6. If the jet is illuminated from behind the page and imaged from the front, the observer should see the gap between the continuous liquid jet and the segment of detached liquid immediately downstream, to identify the breakup location correctly. However, if the jet is illuminated from the left and imaged from the right, the optical path between the illumination source and the camera is blocked by a mass of detached liquid immediately to the right of the breakup location and the gap will not be seen. Instead, a continuous liquid jet will appear, which, in fact, comprises of three distinct liquid masses and the measured breakup length will be considerably longer. For the current example, the measurement error is about 50%.

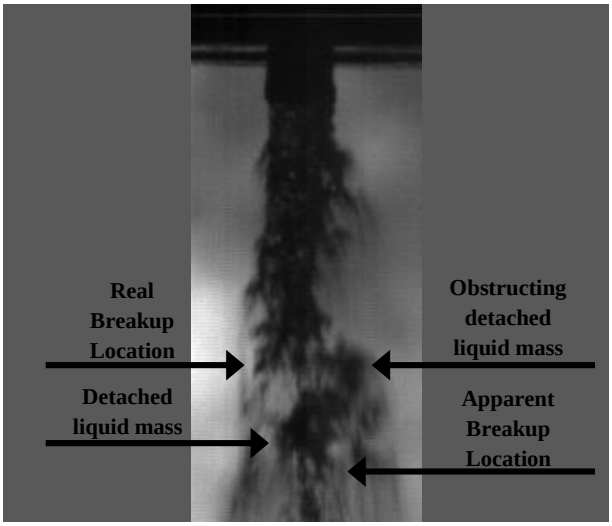

Fig 6. Demonstration of ambiguity of shadowgraphic measurements of breakup length. If the liquid jet is imaged from the left side and recorded at the right side, the detached liquid mass will obstruct the observation of the breakup point and the breakup length will appear about 50% longer than the real value.

The difficulty in the measurement of the breakup length from single images can be alleviated from temporally resolved shadowgraphic images. The uncertainty of the breakup location can be reduced by examining the sequence of the time-dependent images frame by frame. For example, in the first frame of Fig 7, the liquid jet appears to be continuous. However, after 50μs, it is revealed that there is a

discontinuity upstream of the location of the needle, which becomes greater in the subsequent frames, revealing that the liquid is divided in two distinct segments leading to a measured breakup length considerably shorter than identified from the first image.

In summary, shadowgraphy can give accurate measurements of the breakup length provided a temporal record exists. However, the evaluation of the breakup length requires considerable input from the investigator as a frame by frame analysis is required, which is not fully automated and contains a degree of subjectivity.

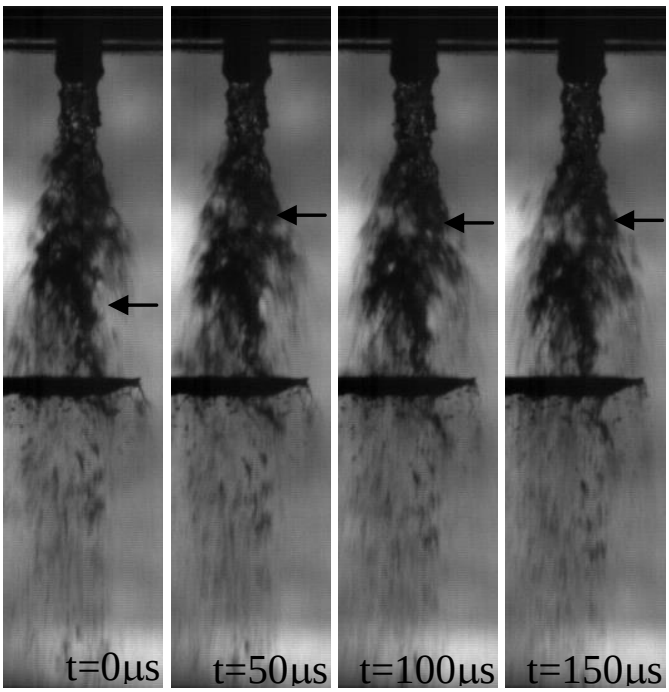

Fig 7. Time resolved imaging reveals the location of liquid jet breaking point, which could be missed by single frame shadowgraphy. The horizontal dark line in the middle of the images is the electrical connectivity probe. The black arrows indicate the location of the liquid jet breakup on each image. (The example shown is for Re=5442, We=526 and MR=171).

3.2. Electrical connectivity

During the application of the electrical connectivity method, the electrical potential is measured between the nozzle and the probe at distinct locations downstream of the nozzle. The location of the liquid jet breakup is determined by analysing the measured potential against the distance from the nozzle. The separation of the continuous liquid jet and the downstream liquid fragments is not always complete. This can be observed in Fig 8 for two flow conditions with different morphological development of the liquid core. In the first case (Fig 8a), close to the breaking point there is a liquid membrane that connects the main jet to the liquid fragment downstream. In the second case (Fig 8b), the vicinity of the breaking point is dominated by ligaments. This has also been observed by [15] for diesel sprays and it was proposed that diesel sprays do not breakup in a single column, but in a number of interconnecting liquid ligaments. While there are differences between the diesel sprays of that study and the air-blast atomiser considered here, the connection between the liquid jet and downstream liquid fragments conducting electricity applies to both cases. For the jets in Fig 8, while the physical connectivity between the liquid jet fragments and the main liquid jet is small, the measured electrical potential is significant (4.1V and 3.9V respectively, with 10V indicating complete discontinuity). Therefore, an appropriate criterion of the measured potential needs to be defined that indicates the location of the breakup even if there is electrical connectivity between the nozzle and the probe.

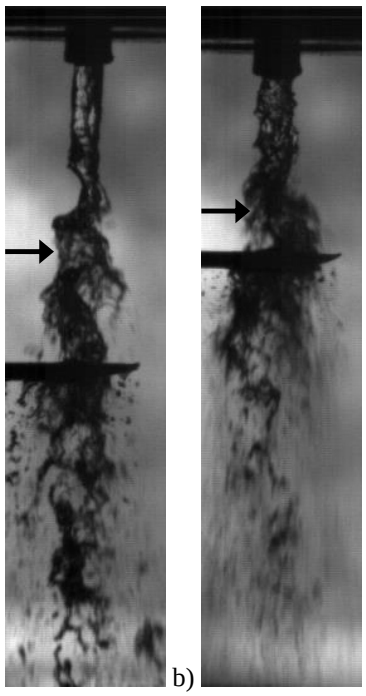

Fig 8. Instantaneous images of the needle probe in contact with the main liquid jet core through minor physical connectivity. a) We=185 b) We=762. The black arrow shows the location of the breakup, which occurs upstream of the location of the needle probe. The respective measured voltages of 4.1 and 3.9V indicate the presence of remaining electrical connectivity.

The breakup criterion is also affected by the change of the measured potential with the apparent contact of the liquid jet on the electrical probe. This is illustrated in Fig 9, which shows a sequence of images of the atomising liquid jet along with the measured voltage drop across the jet nozzle and the probe. The progressively decreasing area of contact between the liquid jet and the needle probe in frames 312 to 320 of Fig 9 shows an increasing trend in the measured voltages between the nozzle and the probe, while in frames 321 to 322 the increasing contact between the jet and the probe decreases the value of the measured voltage. From a low voltage of about 4.5V in frame 312, the measured potential rises to a peak value of about 6V in image 320, where the apparent contact between the jet and the probe is very small.

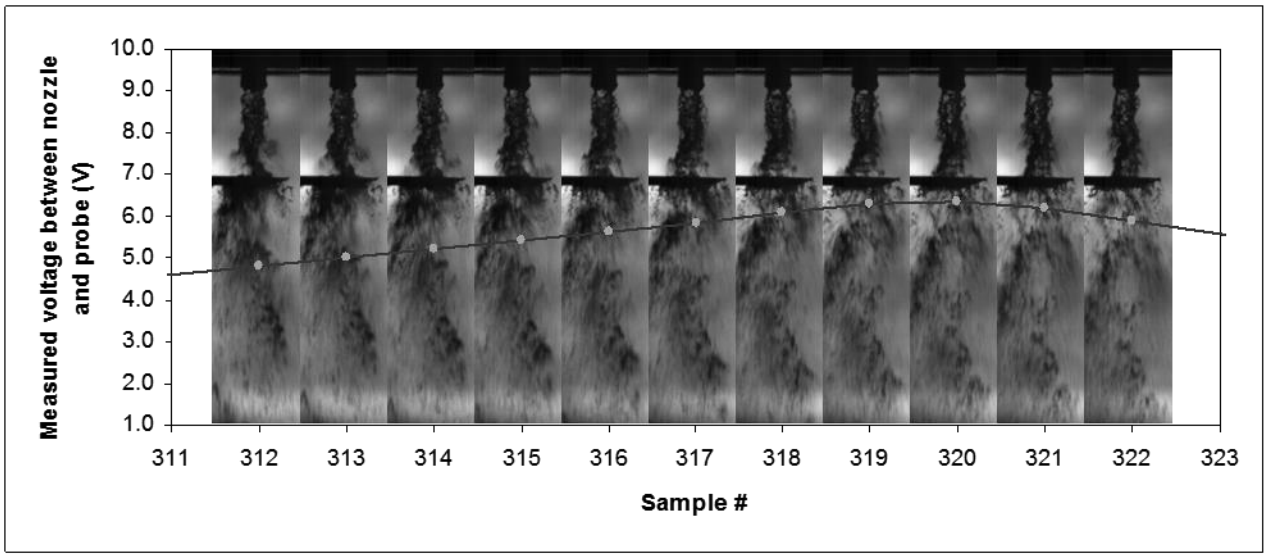

Fig 9. Sequence of temporally resolved shadowgraphic images (We=526 and MR= 171) with the simultaneously measured voltage between the nozzle and the probe (black horizontal line on images) superimposed. The higher voltages indicate lower electrical connectivity.

Since, neither the contact area between the liquid jet and the probe nor the presence of interconnecting ligaments between the main liquid jet and the downstream fragments can be accounted for in the practical application of the technique, the probability function of the measured voltages needs to be considered as a function of the distance from the nozzle. The shape of the probability function is presented in Fig 10, and, as the probe is placed farther from the nozzle, the mean value of the measured voltage increases, the probability peaks at an intermediate location over the range of measured values and the skewness of the histogram shifts from right to left. Therefore, various statistical parameters can be considered to identify the appropriate breaking point criterion for the electrical connectivity technique.

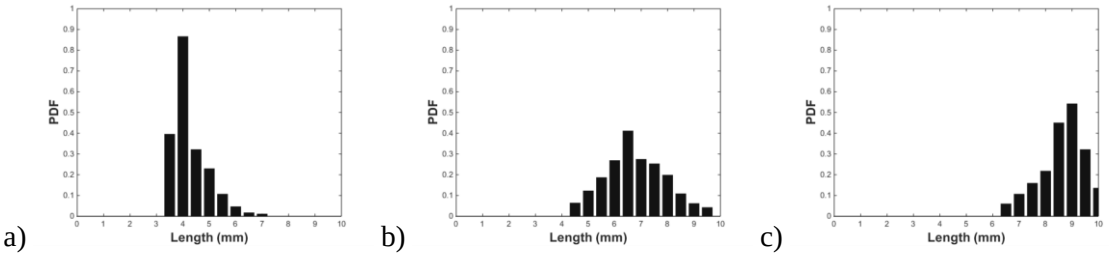

Fig 10. Example of the evolution of the Probability Density Function of the electrical connectivity signal for the flow condition of We=526 and MR=171 when the voltage is measured at a) 11mm, b) 14mm and c) 16mm downstream of the nozzle exit.

The first considered parameter is the mean value of the measured potential between the nozzle and the probe. The mean value of measured voltage is presented in Fig 11 as a function of the distance from the nozzle exit for all the considered flow conditions. In the near nozzle region, the mean measured potential is the same for all cases and its value increases linearly with the distance from the nozzle. The linear increase of the electrical resistance with length is consistent with that of a conductor of constant cross section and indicates that the liquid jet cross section is largely intact for the full length of that region. A linear baseline of the measured potential of the unbroken liquid jet with distance from the nozzle is thus established and is indicated in Fig 11 by a dashed line and is compatible with the behaviour of the potential across a straight conductor with the resistivity of water. The baseline is then used as a guide for the detection of the length of the continuous liquid jet. The results for most flow conditions indicate an initial linear increase of the measured potential with distance from nozzle exit, followed by a sharp increase of the measured potential at a certain distance. This sharp increase can be explained by a sharp decrease of the mean cross section of the liquid jet and is indicative of liquid jet discontinuity. This axial location is marked in Fig 11 with a dot for each flow condition and occurs progressively closer to the nozzle exit as the atomisation improves. All the dots that indicate the jet breakup fall on the baseline established along the length on the intact jet, which indicates that this method of identifying the breakup location with electrical connectivity is independent of the considered flow regimes. Beyond the breakup region, the slope of the mean potential is reduced. This is due to the increasing number of instances, where the maximum value of 10V potential is measured. The advantage of this method for identifying the breakup length is that the average potential provides a clearly defined criterion that is applicable across many flow regimes. The drawback is that the threshold is not fixed and the slope of the voltage with distance needs to be analysed. This may pose difficulties when the slope of the potential does not change dramatically with distance from the nozzle.

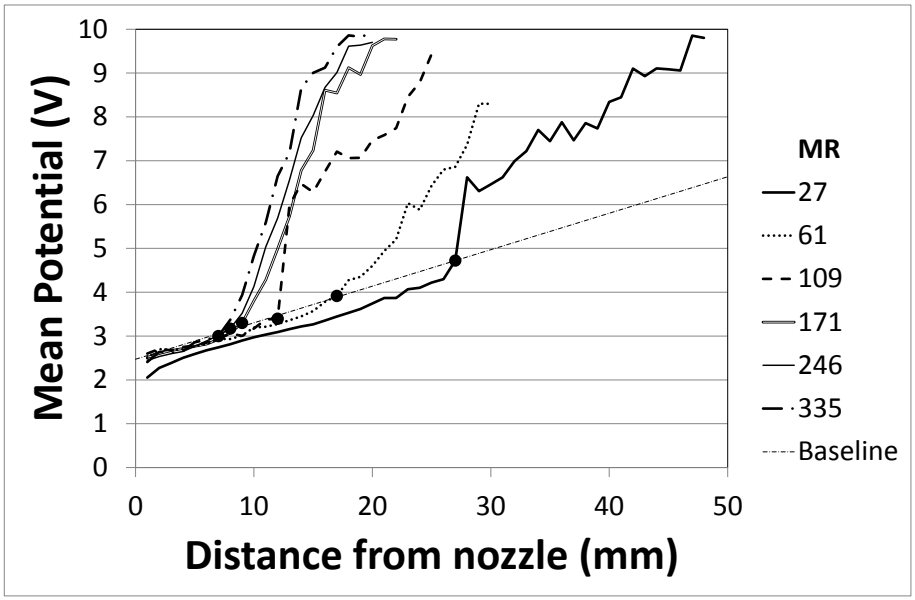

Fig 11. Average values of the measured potential against the distance of the probe from the nozzle exit. The added 'dot' on each line indicates the considered location of the break-up length of the liquid jet for that operating condition.

The second considered parameter is the standard deviation of the fluctuations of the measured potential, which is indicative of the spread of the measured potential values. The evolution of the measured standard deviation with the distance from the nozzle exit is presented in Fig 12 for all flow conditions. The observed general trend is that the standard deviation begins to increase at some location downstream of the nozzle exit and reaches a peak and then decreases again. This behaviour can be explained as follows. Close to the location of the liquid jet breakup, as evaluated from the plot of average measured potential of Fig 11, and marked with a black dot on the standard deviation plots in Fig 12, there is an increase of the fluctuations of the measured voltages due to the formation of a discontinuity of the liquid jet. The black dots fall in the range of 0.2V-0.4V, which appears to be the threshold value for breakup when the standard deviation of the fluctuations of the potential is considered as a criterion. As the probe moves further downstream, greater fluctuations of the measured voltages are measured, since the interconnecting ligaments between the main liquid jet and the downstream liquid fragments become finer. The peak value of the standard deviation identifies the distance where the probe starts to detect complete discontinuity of the liquid jet, meaning that there is no connectivity between the main jet and detached liquid masses even through thin ligaments. As the liquid jet becomes completely discontinuous for most of the time further downstream from the nozzle exit, the fluctuations of the measured potential decrease and tend to zero. Since the threshold value of the standard deviation is not obvious from the trends of Fig 12, the standard deviation of the fluctuations of the measured potential is not a good criterion for detection of the liquid breakup.

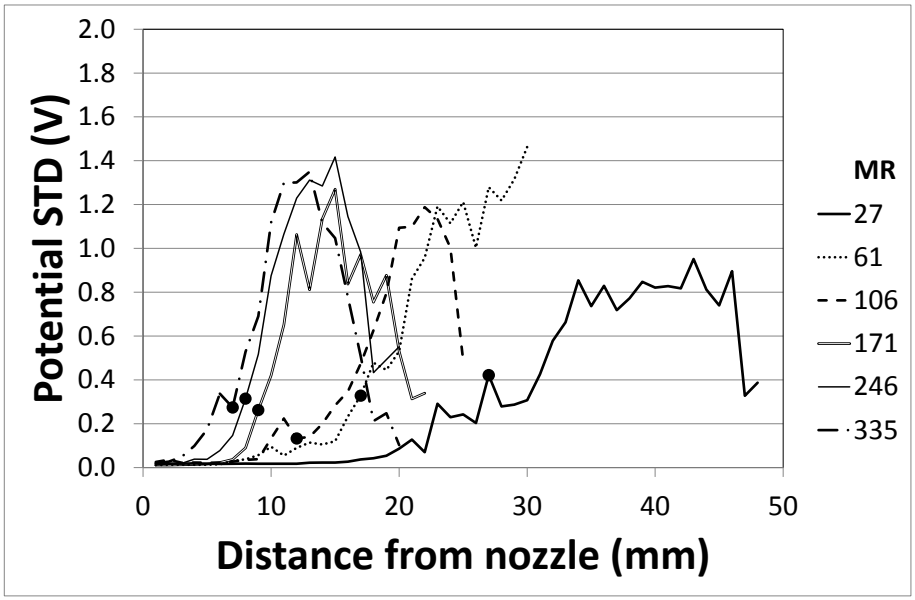

Fig 12. Standard deviation of the fluctuations of the measured potential plotted as a function of the distance of the probe from the nozzle exit. The added 'dot' on each line indicates the considered location of the break-up length of the liquid jet for that operating condition.

The third considered statistical parameter for the interpretation of the measured electrical potential is the skewness of the histogram of the measured potential. While the probe is traversed downstream from the nozzle exit, the skewness of the measured samples changes from positive to negative. This can be observed in Fig 10 for flow We=526 and MR=171 and is similar for all other tested flow conditions. The development of the skewness of the samples of the measured potential is shown in Fig 13 as a function of the distance from the nozzle exit for all flow conditions. Closer to the nozzle, the values of the measured potential are skewed to the right (Fig 10a). This means that, when the breakup of the jet is initiated, it develops fast and there are many samples, where the reduced electrical connectivity of the breaking liquid jet results to high values of measured potential. As the probe is traversed downstream, the probabilities of larger and lower electrical connectivity than that of the liquid jet become equal and the skewness becomes zero (Fig 10b). As the probe is traversed further downstream, the tail of the measured samples will be at low potential values as the electrical connectivity of the liquid jet is diminished (Fig 10c). From the above, it can be asserted that when the liquid jet is discontinuous on average, the skewness of the histogram of the measured values of the potential will be zero. This break-up criterion is easy to apply, because the evaluation of the breakup location is unambiguous and does not require any interpretation of the signal. However, as it will be discussed later the estimated breakup length with this method is considerably longer than what is evaluated when using the other two methods.

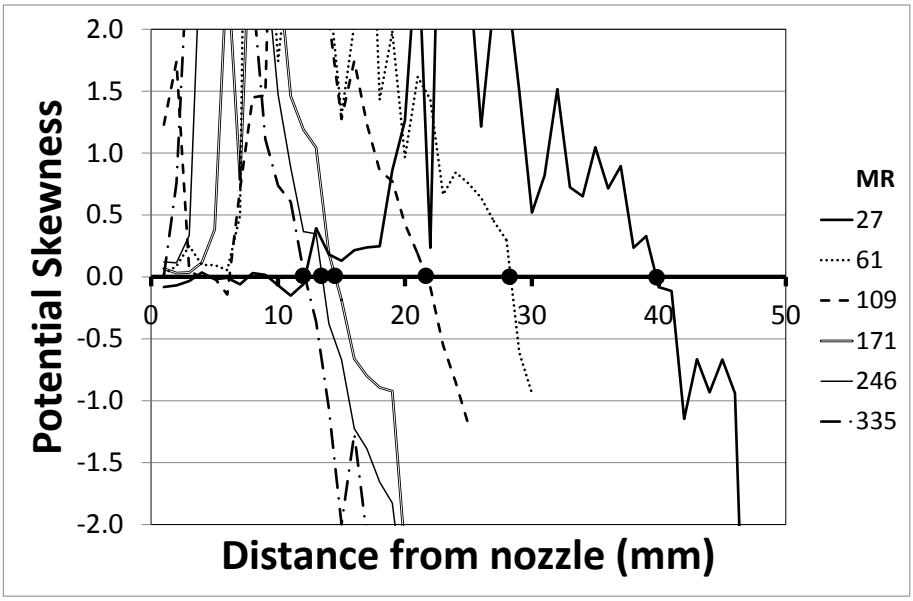

Fig 13. Skewness of the Probability Density Function of the measured potential plotted as a function of the distance of the probe from the nozzle exit for different flow conditions indicated by the MR value. The added 'dot' on each line indicates the considered location of the break-up length of the liquid jet for that operating condition.

Another approach for the evaluation of the average breakup length of the liquid jet may be attempted by considering the fraction of the samples, where the measured potential falls below a certain threshold. In Fig 14, the Cumulative probability Distribution Function (CDF) of the measured potential being below 3.0V, 4.0V, 5.0V, 6.0V, 7.0V 8.0V, 9.0V and 9.9V respectively is presented. Very close to the nozzle exit, the measured potential between the nozzle and the probe is always below the threshold values and therefore the CDF is 0. As the probe moves further away from the nozzle, the CDF increases, signifying the proportion of time that the measured potential is below the selected threshold. Naturally, higher threshold values result to the CDF shifting to greater distances from the nozzle exit. It is difficult to estimate an appropriate threshold just from examining Fig 14. For this reason the value of the potential that corresponds to 50% of the cumulative density function is selected. This represents the median value of the samples and is presented in Fig 15 as a function of the distance from the nozzle exit. Fig 15 shows considerably similar behaviour with Fig 11, which shows that there is a sudden change of the slope of the mean value of the potential with distance from the nozzle exit. The location of the change in the slope is almost identical to that of the mean value of **Fig 11**. This occurs because the distribution of the measured potential is mono-modal and the mean and median values are similar. Therefore, there is no additional information that can be gained from the CDF approach.

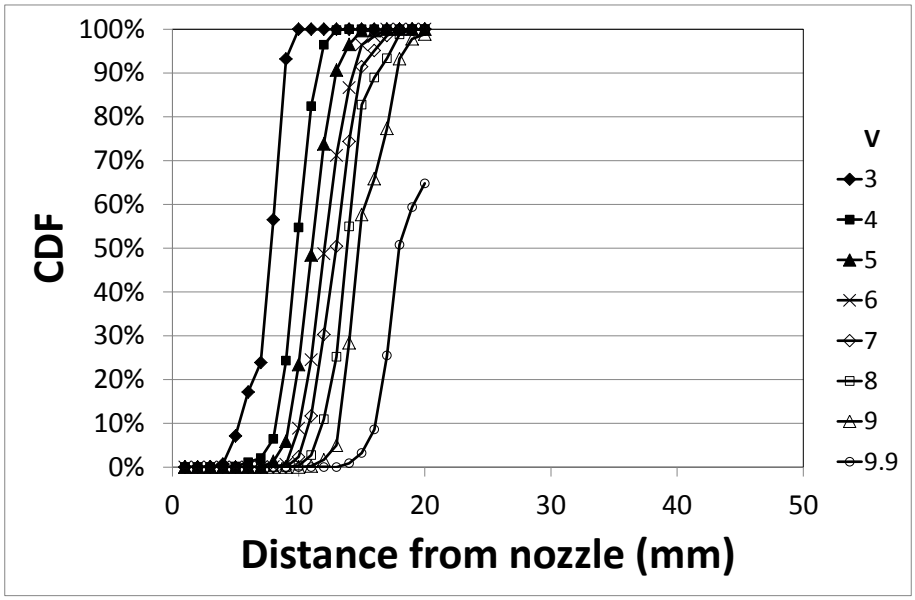

Fig 14. Cumulative Distribution Function (CDF) of the time the measured potential is below a threshold value.

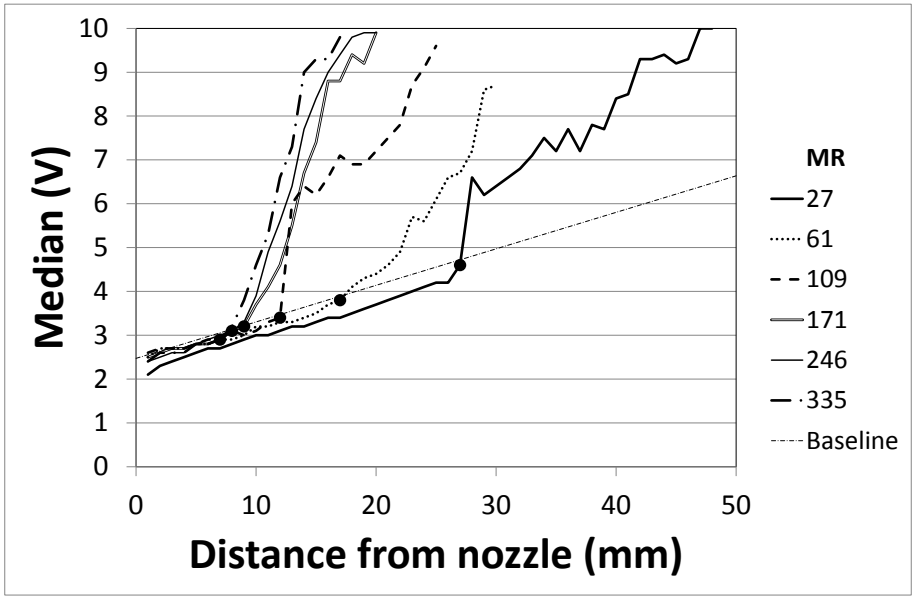

Fig 15. Evaluation of the liquid jet breakup length based on the median value of the measured potential. The added 'dot' on each line indicates the considered location of the break-up length of the liquid jet for that operating condition.

3.3. Optical connectivity

In the optical connectivity technique, unlike shadowgraphy, the main liquid jet can be directly imaged without too much interference from the detached fragments of liquid [16]. This is demonstrated in Fig 16, where an atomising liquid jet was imaged using shadowgraphy and optical connectivity simultaneously. In the shadowgraphic image, all of the liquid phase along the line of sight between the light source and the imaging camera is visualised without distinction between the continuous liquid jet and the surrounding detached liquid. In the image of the optical connectivity technique, only the continuous liquid jet is visualised through which the laser beam propagates.

The interpretation of the shadowgraphic image for the determination of the breakup length is challenging, since both the background and parts of the continuous liquid jet have the same intensity. The interpretation must be based on the change of the image intensity along the boundary of the liquid jet in order to decide which bright image regions are within and which are outside the continuous liquid jet. Such a procedure is complex and automatic image processing is difficult. In the optical connectivity, the liquid phase is clearly seen as bright intensity and the gas phase is clearly seen as dark. Therefore, there is negligible uncertainty at the detection of the location of the continuous liquid phase. Consequently, the breakup length of the liquid jet can be clearly identified. In addition to the breakup length, other useful characteristics of the liquid jet morphology can be identified, such as the wavelength of the interfacial waves and the midline of the liquid jet [31, 32].

The procedure for the processing of the optical connectivity images, a discussion of the advantages and the limitations of the technique for the determination of the breakup length as well as the structure of the liquid jet have been presented elsewhere [16, 33] and only a summary is provided below. The intensity of the fluorescent light is tracked downstream of the liquid nozzle exit. Close to the nozzle exit, the fluorescent intensity remains fairly constant. In the vicinity of the breaking point, there is a sharp reduction of the fluorescent intensity of the liquid jet. The breaking point is identified by considering a threshold value that is a fraction of the intensity at the nozzle exit. This value is in the region of 10%-20% of the fluorescent intensity at the nozzle exit. Since the measured breakup length does not change by more than 10% when changing the value of the above threshold, the determination of the breaking point of the liquid jet is relatively easy and can be performed through automatic image processing which is not susceptible to large uncertainty.

a) 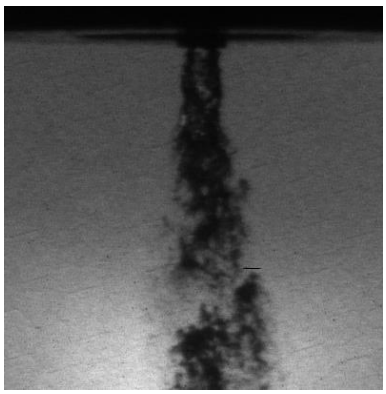 b) 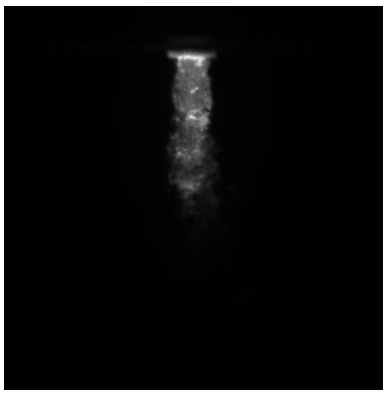

Fig 16. Example of liquid jet visualisation with a) shadowgraphy and b) optical connectivity for operating condition We=526 and MR=171. The optical connectivity technique is less influenced by the products of atomisation around the continuous jet, making the determination of the breakup length easier.

4. Discussion

The comparison of the measurements of the average liquid jet breakup length, obtained with the electrical connectivity technique, high and low speed imaging with shadowgraphy and optical connectivity are presented in Fig 17 as a function of the air-to-liquid momentum ratio (MR).

For all measurements approaches and different processing approaches of each method, with the exemption of the skewness criterion for electrical connectivity, the measurement of the breakup length is within 8-10mm, which corresponds to about $4D_L$. When considering that the average breakup length varies in the range of 25mm to 10mm, depending on flow conditions, the relative uncertainty [34, 35] among the different measuring techniques ranges from ±20% to ±50%, with the uncertainty being more significant for the high MR range, where the average breakup length is shorter. The interpretation of the electrical connectivity measurements with the skewness criterion results to breakup length measurements, which are longer by about 50% than the other methods in most cases. Therefore, this criterion does not provide an accurate evaluation of the breakup length. The interpretation of the results of the remaining methods should be considered with respect to the MR of the measured flow conditions, where the merits and shortcoming of each technique can be highlighted.

For the lower values of the MR range (Fig 17), the atomisation is less intense. In this flow regime, the continuous liquid jet is longer, the shedding of liquid from the surface of the jet is not intense and close to the breakup location there is formation of liquid lamella (Fig 5a-c). For this range of MR, there is good agreement of the measured breakup length among the high and low speed shadowgraphic imaging and the electrical connectivity. The high and low speed shadowgraphic measurements agree well, because the morphology of the jets is such that the liquid jet can be visualised adequately. The good agreement of the electrical connectivity with shadowgraphy for this range of MR values can be hypothesised to be due to the morphology of the constriction of the liquid jet that develops at the breaking point, which is different than the constriction at higher MR values. However, this is a hypothesis and more evidence is required, which can be obtained with high magnification imaging measurements that resolve the morphology of the breaking location better than the resolution used in this study. Considering the optical connectivity technique, the measured breakup length is shorter than for the other techniques. This is explained by Charalampous et al. [16] and is a result of the optical connectivity technique being based on the propagation of a laser beam within the length of a liquid jet in the same way that light propagates in optical fibers. Close to the breaking point the laser beam cannot propagate considerably within the ligaments that connect the continuous core and the downstream liquid jet fragments. As a result, the breakup length measured by the optical connectivity technique will be weighted towards the beginning of the breakup point, while the shadowgraphic techniques will measure a somewhat longer breakup length, since they are more likely to detect the breakup point at a later stage.

For higher values of MR (Fig 17), the atomisation is more intense (Fig 5d-f), and the results show that there is good agreement between optical connectivity and high speed shadowgraphic imaging. Low speed shadowgraphy gives longer breakup lengths and electrical connectivity gives shorter breakup lengths. For low speed shadowgraphy under intense atomisation, due to visual interference of the breakup location from droplets and liquid fragments, it is more difficult to identify the breakup location correctly. Therefore, the measured breakup length can appear longer. However, when using high speed shadowgraphy, the temporal record of the acquired images can help to overcome the interference from the detached liquid segments by tracking the discontinuity upstream in the liquid jet. In the optical connectivity method, since the laser beam is introduced through the nozzle and only the main liquid jet is illuminated, optical interference with the surrounding droplets is avoided. Additionally, as the breakup length is naturally short under intense atomisation, the losses of the laser beam intensity along the interface of the continuous liquid jet due to refraction are small and the illumination of the continuous jet is complete. The shorter breakup length detected by electrical connectivity might be attributed to the nature of the technique. As the probe is physically inserted into the flow, electrical connectivity will be able to detect the narrowing of the continuous jet close to the nozzle. However, at high MR, the flow is fast and the narrowing does not have sufficient time to develop to a discontinuity within the probe location indicating a short breakup length. Overall, confidence in the measurement of the breakup length for the region of higher MR is higher for the high speed shadowgraphy and the optical connectivity, while electrical connectivity has greater uncertainties.

Overall, when considering the 3 most reliable measurement methods of the breakup length, namely optical connectivity, high speed shadowgraphy and electrical connectivity interpreted according to the mean value of the measured potential, the maximum measurement error among them is within ±15% of the mean measured value. This range is much narrower than the ±50% range for all the measurement techniques and processing approaches considered.

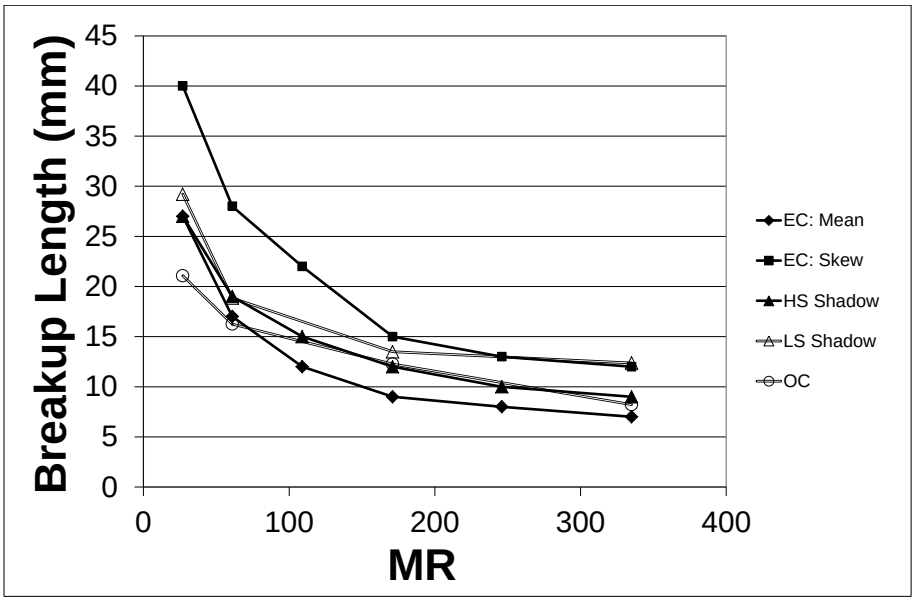

Fig 17. Comparison of the breakup length measurements obtained by the three experimental techniques. Each technique is indicated as EC Mean: Electrical Connectivity using the mean criterion (♦), EC Skew: Electrical Connectivity using the Skewness Criterion (■), HS Shadow: High Speed Shadowgraphy (▲), LS Shadow: Low Speed Shadowgraphy (△) and OC: Optical Connectivity (○).

From an application point of view, the selection of the appropriate technique depends on the implementation of the experiment and the results, which are sought. The most common way to measure the breakup length is low speed shadowgraphy. It has the advantages that it is non-intrusive, very easy to set up and requires equipment that is available at all laboratories. There is no limit on the length of the breakup length that can be measured and, in addition, valuable information can be extracted regarding the overall atomisation process and the behaviour of the detached liquid segments. On the downside, shadowgraphy requires optical access to the atomising spray from two opposite sides, one for the illumination and one for the imaging system, which could be a problem when the spray is contained. Also, the analysis of the images is susceptible to the subjective interpretation of the researchers, since the location of the breakup point must be determined visually. This is a significant issue when atomisation is intense and there is no clear view of the liquid jet and therefore there is ambiguity in the measurements. This ambiguity can be overcome by using high speed shadowgraphy. The setup remains essentially the same, but the cost of the required imaging system is much higher and may not be available at all laboratories. In this case, however, the analysis of the shadowgraphic record requires substantial user effort, as the breakup location needs to be traced upstream which needs to be done manually. In general, shadowgraphy is a good tool for the overall investigation of the

liquid jet breakup with some limitations depending on the atomisation intensity, which can be overcome with temporally resolved measurements.

The optical connectivity approach for the measurement of the liquid breakup length is most appropriate when there is optical obstruction of the liquid jet from surrounding detached liquid fragments, since it visualises only the main jet. This is particularly important for cases where many droplets surround the liquid jet core. The optical connectivity images of the liquid jet present clearly the continuous liquid jet. This makes the determination of the breakup length straightforward by tracing the fluorescent intensity along the jet length, which is an advantage over shadowgraphy and can be performed with automatic image processing. Additional information can also be extracted for the overall morphology of the liquid jet, since the full image of the continuous jet is obtained [31, 32]. The technique does pose increased demands on equipment compared to shadowgraphy because a laser source is required for illumination. However, lasers are available at most laboratories studying atomisation. Another difficulty is that the atomiser must be modified, so that the laser beam can be guided through the nozzle. In case of complex atomiser designs, this might not be possible. Finally, it has been shown that there will be a decrease of the laser beam intensity as it propagates along the liquid jet length due to refraction [16] at the liquid interface. Therefore, this technique is recommended for cases where the breakup length is expected to be short, which are related to intense atomisation and, therefore, for most practical applications. This is also the case when low speed shadowgraphy becomes problematic. Therefore, the two techniques can be complementary.

Finally, the electrical connectivity technique is an alternative method to optical approaches and is dedicated to the measurement of the breakup length. This technique is attractive, since it is easy to set up, has little demand on equipment and produces small datasets. Like shadowgraphy, there is no limitation of the maximum breakup length that can be measured. The drawbacks of the technique are that the estimated breakup length can be somewhat shorter than what is measured by optical techniques. This is due to the interpretation of the measured potential between the nozzle and the probe. The requirement for physical access to the near nozzle region may be a problem for some applications, especially in limited spaces and in physically hazardous environments, where the direct contact of the spray with the probe can cause damage or contamination of the surface that would alter the electrical resistance of the probe and interfere with the measurement. The time required to characterise a single flow condition is also longer compared to other techniques, since the probe has to be traversed along the jet. Finally, a requirement of the technique is that the liquid must be electrically conductive. Overall this technique is promising when only the breakup length is required and demands on equipment needs are minimal.

The advantages and disadvantages of the considered techniques are summarised in Table 2.

Table 2. Summary of advantages and disadvantages of examined methods for measurements of liquid jet breakup length

Method	Advantages	Disadvantages
Shadowgraphy	• Non-intrusive • Easy to set up • Can measure jet morphology and spray patterns	• Measurement bias when not time-resolved • Measurement is susceptible to interpretation • Two way optical access (one for camera, one for illumination)
Electrical Connectivity	• Easy to set up • Economic • Small datasets	• Time consuming scanning required • Physically intrusive probe • Only measures breakup length
Optical Connectivity	• Clear separation of continuous liquid jet and gas phase • Suppresses interference of liquid droplets and fragments around continuous liquid jet • Can measure continuous liquid jet morphology • Feasible with equipment available in most laboratories	• Modification of atomiser is required • Limitation of maximum breakup length • Two way optical access (one for camera, one for illumination)

5. Conclusions

A comparative investigation of the measurement of liquid jet breakup length of a co-axial airblast atomiser was conducted using electrical connectivity, optical connectivity and shadowgraphy for a range of flow conditions with air-to-liquid Momentum Ratios (MR) between 27 and 335 and momentum flux ratios between 0.67 and 8.27. The findings are as follows:

During shadowgraphic measurements, the optical access to a central liquid jet is obstructed by the presence of detached liquid segments along the line of sight between the jet and the camera resulting to bias towards long breakup length measurements. High speed shadowgraphy provides the temporal evolution of the liquid jet, which can alleviate some of the uncertainty in the interpretation of the shadowgraphs and produce more reliable breakup length measurements.

The electrical connectivity technique was affected by the presence of thin liquid ligaments that interconnect the detached liquid fragments and are sufficient to allow the conduction of electricity. Different criteria for processing the measured values of potential in order to identify the breakup length were considered, which were assisted from the availability of understanding gained from simultaneous electrical connectivity and shadowgraphic measurements. The criteria included the mean value of the measured potential, its standard deviation, its skewness and its median value. The methods, based on the mean and the median value of the potential, were appropriately reliable to measure the mean value of the breakup length, but they have to be evaluated at different injector geometries. Therefore, if an appropriate criterion to process the electrical connectivity potential measurements is used, the measured breakup length is within the same range of the other techniques.

The optical connectivity technique can overcome the optical obstructions caused by droplets surrounding the liquid jet, which become more significant with the increase of Momentum Ratio of the flow conditions.

Overall, it is found that the three methods have merits and should be used complementary depending on the requirements of the investigation and the morphology of the investigated liquid jets. If applied correctly, the maximum measurement error between the techniques is within ±15% of the mean value of the breakup length.

6. Acknowledgements

The research was supported by the UK Engineering and Physical Sciences Research Council (EPSRC) grant EP/G01597X/1 and the European Office of Aerospace Research and Development (EOARD) contract FA8655-09-1-3036.

References

[1] A.H. Lefebvre, Atomization and sprays, Hemisphere Publishing Corporation, 1989.
[2] L. Bayvel, Z. Orzechowski, Liquid atomization, Taylor & Francis, 1993.
[3] P.H. Marmottant, E. Villermaux, On spray formation, Journal of Fluid Mechanics, 498 (2004) 73-111.
[4] G.N. Laryea, S.Y. No, Spray angle and breakup length of charge-injected electrostatic pressure-swirl nozzle, Journal of Electrostatics, 60 (2004) 37-47.
[5] K. Sallam, C. Aalburg, G. Faeth, Breakup of round nonturbulent liquid jets in gaseous crossflow, Aiaa J, 42 (2004) 2529-2540.
[6] H. Eroglu, N. Chigier, Z. Farago, Coaxial Atomizer Liquid Intact Lengths, Physics of Fluids A-Fluid Dynamics, 3 (1991) 303-308.
[7] F. Xiao, M. Dianat, J.J. McGuirk, LES of turbulent liquid jet primary breakup in turbulent coaxial air flow, Int J Multiphas Flow, 60 (2014) 103-118.
[8] J.C. Lasheras, E. Villermaux, E.J. Hopfinger, Break-up and atomization of a round water jet by a high-speed annular air jet, Journal of Fluid Mechanics, 357 (1998) 351-379.
[9] C. Engelbert, Y. Hardalupas, J.H. Whitelaw, Breakup Phenomena in Coaxial Airblast Atomizers, Proceedings of the Royal Society of London Series A, Mathematical and Physical Sciences, 451 (1995) 189-229.
[10] A.J. Yule, I. Filipovic, On the Break-Up Times and Lengths of Diesel Sprays, International Journal of Heat and Fluid Flow, 13 (1992) 197-206.
[11] M. Ochowiak, L. Broniarz-Press, S. Rozanska, Analysis of Liquid Jet Breakup in One- and Two-Phase Flows, Chemical Engineering & Technology, 35 (2012) 1685-1691.
[12] G.S. Settles, Schlieren and Shadowgraph Techniques: Visualizing Phenomena in Transparent Media, Springer Berlin Heidelberg, 2001.
[13] H. Hiroyasu, M. Shimizu, M. Arai, The breakup of high speed jet in a high pressure gaseous atmosphere, ICLASS-82, 1982.
[14] B. Chehroudi, S.H. Chen, F.V. Bracco, On the intact core of full-cone sprays, SAE Technical Papers 850126, (1985).
[15] A.J. Yule, D.G. Salters, A Conductivity Probe Technique for Investigating the Breakup of Diesel Sprays, Atomization Spray, 4 (1994) 41-63.
[16] G. Charalampous, Y. Hardalupas, A.M.K.P. Taylor, Novel Technique for Measurements of Continuous Liquid Jet Core in an Atomizer, Aiaa J, 47 (2009) 2605-2615.
[17] G. Charalampous, Y. Hardalupas, A. Taylor, Structure of the continuous liquid jet core during coaxial air-blast atomisation, Int J Spray Combust, 1 (2009) 389-415.
[18] D. Colladon, On the reflections of a ray of light inside a parabolic liquid stream, Comptes Rendus, (1842) 800-802.
[19] D. Colladon, La Fontain Colladon, La Nature, (1884) 325-326.
[20] L.A. Melton, C.W. Lipp, Criteria for quantitative PLIF experiments using high-power lasers, Exp Fluids, 35 (2003) 310-316.
[21] G. Charalampous, C. Hadjiyiannis, Y. Hardalupas, Numerical and experimental investigation of the optical connectivity technique in cross flow atomization, 12th International Conference on Liquid Atomization and Spray Systems, Heidelberg, Germany, 2012.
[22] G. Charalampous, N. Soulopoulos, Y. Hardalupas, Ray tracing analysis of realistic atomizing jet geometries for optical connectivity applications, 53rd AIAA Aerospace Sciences Meeting, American Institute of Aeronautics and Astronautics, AIAA 2015-0164, 2015.
[23] W.Y. Cai, C.F. Powell, Y. Yue, S. Narayanan, J. Wang, M.W. Tate, M.J. Renzi, A. Ercan, E. Fontes, S.M. Gruner, Quantitative analysis of highly transient fuel sprays by time-resolved x-radiography, Applied Physics Letters, 83 (2003) 1671-1673.
[24] M.J. Renzi, M.W. Tate, A. Ercan, S.M. Gruner, E. Fontes, C.F. Powell, A.G. MacPhee, S. Narayanan, J. Wang, Y. Yue, R. Cuenca, Pixel array detectors for time resolved radiography (invited), Review of Scientific Instruments, 73 (2002) 1621-1624.
[25] Y. Yue, C.F. Powell, R. Poola, J. Wang, J.K. Schaller, Quantitative measurements of diesel fuel spray characteristics in the near-nozzle region using X-ray absorption, Atomization Spray, 11 (2001) 471-490.
[26] M. Linne, M. Paciaroni, T. Hall, T. Parker, Ballistic imaging of the near field in a diesel spray, Exp Fluids, 40 (2006) 836-846.
[27] M.A. Linne, M. Paciaroni, J.R. Gord, T.R. Meyer, Ballistic imaging of the liquid core for a steady jet in crossflow, Appl Optics, 44 (2005) 6627-6634.
[28] M. Paciaroni, M. Linne, Single-shot, two-dimensional ballistic imaging through scattering media, Appl Optics, 43 (2004) 5100-5109.

[29] M. Paciaroni, M. Linne, T. Hall, J.P. Delplanque, T. Parker, Single-shot two-dimensional ballistic imaging of the liquid core in an atomizing spray, Atomization Spray, 16 (2006) 51-69.
[30] J.-P. Matas, A. Cartellier, Flapping instability of a liquid jet, Comptes Rendus Mécanique, 341 (2013) 35-43.
[31] C. Hadjiyiannis, S. Sahu, G. Charalampous, Y. Hardalupas, A.M.K.P. Taylor, Correlation Between the Primary Break-up of Liquid Jets and Downstream Spray Characteristics in Air-blast Atomizers, 6th European Combustion Meeting ECM 2013, Lund, Sweden, 2013.
[32] G. Charalampous, Y. Hardalupas, C. Brown, U. Mondragon, V. McDonell, Investigation of injection characteristics of alternative aviation fuels by Laser-Induced Fluorescence imaging, 51st AIAA Aerospace Sciences Meeting including the New Horizons Forum and Aerospace Exposition, AIAA 2013-0162, American Institute of Aeronautics and Astronautics, 2013.
[33] G. Charalampous, C. Hadjiyiannis, Y. Hardalupas, Proper Orthogonal Decomposition analysis of photographic and optical connectivity time resolved images of an atomising liquid jet, 24th Annual Conference on Liquid Atomization and Spray Systems, Estoril, Portugal, 2011.
[34] S. Tavoularis, Measurement in Fluid Mechanics, Cambridge University Press, 2005.
[35] L. Kirkup, Experimental Methods: An Introduction to the Analysis and Presentation of Data, Wiley, 1996.